Negative capacitance in doped bi-layer organic light-emitting devices*

Li Nuo(李 诺), Gao Xin-Dong(高歆栋), Xie Zuo-Ti(谢作提),
Sun Zheng-Yi(孙正义), Ding Xun-Min(丁训民), and Hou Xiao-Yuan(侯晓远)†

Surface Physics Laboratory (National Key Laboratory), Fudan University, Shanghai 200433, *China*

(Received 9 September 2010; revised manuscript received 25 September 2010)

This paper reports that the doped bi-layer organic light-emitting devices are fabricated by doping in different regions of the light-emitting layer, the admittance and luminance spectra to characterize the capacitance and luminance of the device are measured. Negative capacitance (NC) appeared at low frequencies when the doped devices are biased with high voltages. The measured phase difference between AC voltage applied across the device and AC current flowing through the device show that the device is inductive when NC appears.

Keywords: negative capacitance, doping in different regions, organic light-emitting device

PACS: 73.61.Ph, 78.60.Fi, 78.66.Qn **DOI:** 10.1088/1674-1056/20/2/027306

1. Introduction

The analysis of space charge distribution in the organic layers is an important topic in the field of organic light-emitting devices (OLEDs). Generally, measuring the differential capacitance characteristics of devices is an effective method for the topic. Some factors affecting space charge distribution, such as trap states,[1] interfacial charges,[2−5] carrier mobility[6] and space charge distribution[7] in the devices, can be characterized by measuring the device's capacitance.

Usually OLEDs show negative capacitance (NC), i.e. with the change of bias and frequency the measured differential capacitance of the device changes from positive to negative. Currently, there exist many viewpoints on the mechanism of NC. Gommans *et al.* suggested that NC might originate from the capacitance deviation (ΔC) from the geometric capacitance of the device, due to the distribution of space charges in the device.[8] Bisquert *et al.* considered that NC might be attributed to the effect of interfacial states at the cathode/organic interface on electron injection, according to the study of polymer devices with different metal cathodes.[2,9] And, Ehrenfrenund *et al.* reported that the time-dependent recombination of holes and electrons would be the main origin of NC.[10,11] All the proposed mechanisms of NC mentioned above are based on the research of polymer devices. By contrast, for the small molecular OLEDs, NC is usually illustrated by two different viewpoints as follows: one claimed that NC was attributed to inductance-like effect originating from accumulation and recombination of carriers near the organic/organic interface and transport of minority carrier in the device;[12−16] the other considered that NC was rooted in the dynamic effect of energy distribution about occupancy/release of interfacial states at the electrode/organic interface.[17,18] Both these two viewpoints emphasized dominance of the factor chosen in the mechanism of NC. Specially, in order to prove that NC was produced by interfacial states at the electrode/organic interface, Garcia-Belmonte *et al.* fabricated electron-only and hole-only devices and obtained NC results at low frequencies from 0.4 Hz to 4 Hz. It seemed that the viewpoint of carrier recombination induced NC could be discarded. But this may not be the case for bi-carrier devices.

We fabricate devices with different space charge distributions in organic layers but the same electrode/organic structure via doping diabetic cardiomyopathy (DCM) molecules into different regions of the tris-(8-hydroxyquinalato) aluminum (III) (Alq_3) emitting layer in the bi-layer OLEDs. The luminance characteristic of the device is affected by the different doping regions, and then it results in the change of NC. It

*Project supported by the Natural Science Foundation of the Shanghai Committee of Science and Technology, China (Grant No. 08JC1402300).

†Corresponding author. E-mail: xyhou@fudan.edu.cn

© 2011 Chinese Physical Society and IOP Publishing Ltd

is, therefore, demonstrated that the dominant factor of mechanism on NC in the bi-carrier device should still be transportation, distribution and recombination of the carriers. In addition, the phase difference between AC voltage applied across the device and corresponding AC current is measured. Comparison of the phase difference with the NC appearing in capacitance-frequency (C–F) characteristic indicates that the device turns from capacitive to inductive with decreased frequency and high bias. The NC and inductive characteristic of device exhibit similar features on frequency. They are in accordance with each other.

2. Experiment

We have fabricated N,N-bis(l-naphthyl)-N,N-diphenyl-1,1-biphenyl-4,4 –diamine (NPB)/Alq_3 bilayer doped devices with three different structures: Type A (doping near the organic/cathode interface): ITO\NPB (40 nm)\$Alq_3$ (60 nm)\$Alq_3$: DCM (20 nm, 1%)\LiF (1 nm)\Al (80 nm); Type B (doping in the middle of the emitting layer): ITO\NPB (40 nm)\$Alq_3$ (30 nm)\$Alq_3$:DCM (20 nm, 1%)\$Alq_3$ (30 nm)\LiF (1 nm)\Al (80 nm); Type C (doping near the organic/organic interface): ITO\NPB (40 nm)\$Alq_3$: DCM (20 nm, 1%)\$Alq_3$ (60 nm)\LiF (1 nm)\Al (80 nm). The doping concentration of these doped devices was all 1%. Besides, undoped devices of Type D: ITO\NPB (40 nm)\$Alq_3$ (80 nm)\LiF (1 nm)\Al (80 nm) were also fabricated as reference devices. The schematic diagram of device structure is shown in Fig. 1. All the layers were deposited in a vacuum chamber with base pressure of 1×10^{-5} Pa.

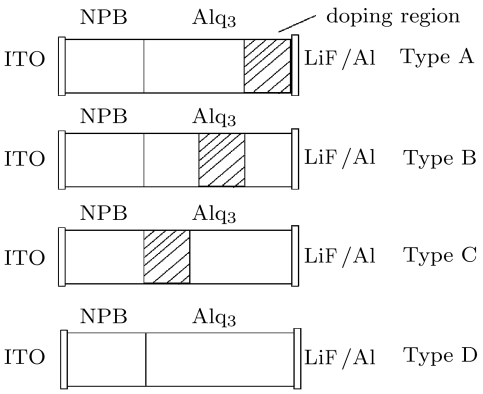


Fig. 1. Schematic diagram of device structure.

The L–V characteristics of the devices were measured by a luminance meter and a remote controlled Keithley 236 source. The measurement of capacitive characteristics was mainly carried out with an LCR analyser (HP4284A). The AC phase difference was measured by a Lecory LT262 oscilloscope and a Tektronix AFG3101 function generator. All the measurements were conducted at room temperature. Many individual devices of each type were measured and the data were averaged over all the measured devices.

3. Results and discussion

Figure 2 shows the capacitance–voltage (C–V) relations of the doped and undoped devices. The bias ranges from 0 V to 12 V while the AC frequency is kept at 5 kHz. It can be seen in the figure that below 4 V the capacitance keeps almost unchanged with bias (the variation of capacitance with bias is less than 0.05 nF), and the difference between the capacitances of doped and undoped devices, denoted as additional capacitance $C_{\rm tr}$ hereafter, is approximately 0.8 nF, which is mainly attributed to the trapped charge due to doping while the structural difference of the doped devices results in a very small capacitance difference of about 0.1 nF only. Moreover, the capacitance decreases with increasing bias in the range from 4 V to 12 V, regardless of the device structure. As shown in Fig. 2, the capacitance of devices of Type A, in which the doped region is near the organic/cathode interface, only changes 0.5 nF over the bias range from 0 V to 12 V. In the same bias range, the device capacitance of Type B, in which the doped region is at the middle of the emitting layer, decreases by about 0.8 nF,

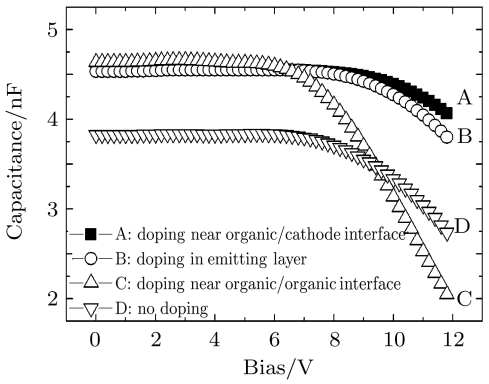


Fig. 2. The capacitance–voltage (C–V) characteristics measured at 5 kHz.

while the device capacitance of Type C which is doped near the organic/organic interface decreases by 2.6 nF over the same range of bias. Therefore, in doped devices, the shorter the distance between the doped region and organic/organic interface is, the larger the

decrease of capacitance will be. Meanwhile the capacitance of undoped devices decreases by 1.2 nF in the whole bias range. In brief, the capacitance of the devices decreases with bias, and the decrement enlarges in the order of device Types A, B, D and C.

The C–V characteristics at a frequency of 500 Hz of the four types of devices are shown in Fig. 3. Compared with the results at 5 kHz shown in Fig. 2 where all the capacitances are positive, the capacitance decreases with bias more obviously, reaching 1.4 nF, 3 nF, 10 nF and 7 nF for the devices of Types A, B, C and D respectively. The capacitances start to vary with bias when the biases of four devices are about 7.2 V, 6.0 V, 4.8 V and 4.6 V respectively. Remarkably, devices C and D show NC in the high bias range from 10 V to 12 V. The present experimental results of C–V characteristics indicate that bi-layer small molecular OLEDs will show NC when the devices operate under high biases and at low frequencies. The NC is not observed for devices A and B over the same bias range. Possibly it might emerge under even higher bias. (The bias higher than 12 V will damage the devices. Therefore the highest bias in the present experiment is set as 12 V.)

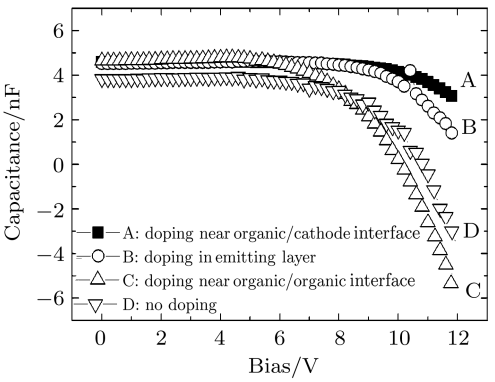


Fig. 3. The C–V characteristics measured at 500 Hz.

Figure 4 shows the L–V characteristics in the same bias range (0 V–12 V) for illustrating the relation between NC and radiative recombination of the carriers (luminance). As one may see, when the bias is below 4 V, the luminance intensity in all the four cases remains at almost zero, unchanged with bias. They start increasing with bias from 4 V. The increment of intensity enlarges in the order of device Types A, B, D and C. Comparing Fig. 3 with Fig. 4, one may see that the intensity begins to enhance when the device is turn-on (the turn-on voltage is defined as that corresponding to the luminance of 1 cd/m^2 in Fig. 4) and the capacitance starts to decrease at the same bias accordingly. And the order of enhancement in intensity is consistent with the decrement in capacitance in those devices.

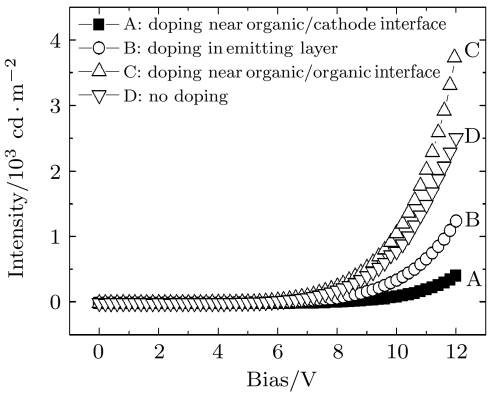


Fig. 4. The L–V characteristics of four different devices.

The region-dependent effect of doping on the capacitance and the luminance characteristics is obviously due to the DCM molecules doped in the Alq_3 layer. They may result in three factors: electron trap,[19] enhancement of yield and additional capacitance.

First, the additional field produced by the trapped electrons builds up the redistribution of field in organic layers. The redistributed field affects the carrier injection, transport and the space charge distribution and then the electric characteristics of the device. For example, in device of Type A, the trapped electrons introduced by doping near the organic/cathode interface enhance the barrier of electron injection at the cathode/organic interface, resulting in unbalanced carrier injection. But in the devices of Types B and C, the field introduced by the trapped electrons has weaker effect on the electron injection because of the larger distance between the doped region and cathode than that in device of Type A.

Secondly, the doped DCM molecules can enhance yield and increase brightness by energy transfer of excitons after the devices are turn-on. It is well known that excitons are produced at the organic/organic interface and then diffuse from the interface to the interior of the Alq_3 layer in an NPB/Alq_3 bi-layer device. And the concentration of excitons reduces from the organic/organic interface to the inside of the Alq_3 layer. So the intensity of Type C device doped near organic/organic interface is larger than other types of devices. Its spectrum shows simple DCM luminance characteristics. By contrast, two types of luminance, DCM and Alq_3, exist in the spectrum of Type B, though the distance between the doping regions and

the organic/organic interface is larger than the sum of diffusion length of Alq_3[20,21] and energy transfer radius of DCM-Alq_3 system[22−24] in Type B devices. In addition, the luminance of Type A is the weakest in all types of devices and its spectrum shows peak of Alq_3 only. So the doped DCM molecules work as electron traps mainly in Type A and Type B.

Thirdly, the additional capacitance is produced after electrons are trapped by DCM molecules in the device. Prior to the turn-on of the device, the carriers injected into the device arrive at the organic/organic interface and accumulate near the interface. Therefore, the density of electron near the interface is higher than those in the other two doping regions, and then the dopants capture more electrons in Type C devices. So the additional capacitance of Type C is larger than $C_{\rm tr}$ of Types A and B by about 0.1 nF when the bias is lower than the voltage of device turn-on.

After the device is turn-on, because the hole mobility in the NPB layer is much larger than the electron mobility in the Alq_3 layer, the holes accumulate at the organic/organic interface before the electrons arrive at there. The accumulated holes redistribute the internal field, weaken the hole injection and transport, enhance the electron transport until the electrons reach the interface, recombine with the holes and reduce accumulation of the holes. After a relaxation process, a stable state is formed. So there is an obvious lag between the AC voltage and the corresponding space charge distribution, producing an inductance-like effect. This effect is demonstrated as negative contribution of capacitance $C_{\rm n}$. It is noticeable in Figs. 3 and 4 that $C_{\rm n}$ is closely associated with luminance. The more luminance gives off, the larger $C_{\rm n}$ is. So the capacitance change of undoped devices of Type D, for which the luminance is less than Type C only, is more obvious than that of Type B and Type A.

The presence of the inductance-like effect can be checked by measuring the phase difference between AC voltage across the two sides of the device and AC current through it. Figure 5 shows the phase difference–frequency (ϕ–F) relations in the frequency range from 20 Hz to 1 kHz under the 12 V bias. It is immediately evident that all phase differences of the devices are positive, i.e. the inductive character is stronger than the capacitive character, when the frequency is lower than 60 Hz. The inductive character of Type C device is the strongest, while that of Type A is the weakest. In addition, the phase difference decreases with increasing frequency. It changes from positive to negative, i.e., the device switches from inductive to capacitive. And the capacitive enhancement is related to the device structure. The capacitive character of the device weakens with the doping region varying from near the organic/cathode interface to near the organic/organic interface at the same frequency. For example, at the frequency of 200 Hz, the phase differences of Types A, B and C are $-9\times10^{-3}\pi$, zero and $9\times10^{-3}\pi$, respectively, corresponding to capacitive, neither capacitive nor inductive and inductive. The last one may also named as "negative capacitive". Moreover, the phase difference of the devices approaches to a constant with increasing frequency.

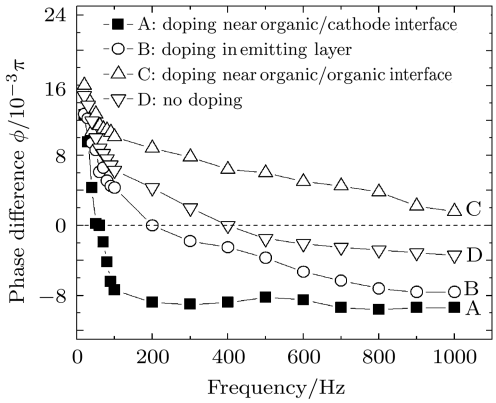


Fig. 5. The phase difference–frequency (ϕ–F) characteristics measured under 12 V bias.

The results of capacitance–frequency (C–F) characteristics measured in the same condition are shown in Fig. 6. It can be seen that the capacitance of the devices increases with the frequency. All the devices exhibit NC below 60 Hz, for which Type C is the strongest and Type A the weakest. So the absolute value of NC is doping-region-dependent, too. The devices of Type C exhibit NC in the whole frequency region from 20 Hz to 1 kHz, while the undoped devices of Type D show capacitive characteristic in between Type C and Type B. Moreover, the capacitance of the devices approaches to a constant with increasing frequency, too.

Comparing ϕ–F relations in Fig. 5 with C–F characteristics in Fig. 6, one can see that the phase difference and capacitive characteristics at the same frequency are in accordance with each other. That is to say, the whole device is inductive when the phase difference is positive, which corresponds to the NC state, and *vice versa*. It is thus clear that NC originates from the inductive behaviour of the devices. When the luminance is weak, there exists distinct unbalance of carrier injection/transport and the accumulation of holes, which blocks the hole transport

and enhances the electron transport in organic layers, is dominant. So it decreases the relaxation time, reduces the phase difference and weakens the inductive character. When the luminance is strong enough, the carrier injection/transport is more balanced than that in the weak luminance situation and the effect on carrier transport due to the accumulation of holes decreases. So the relaxation time increases and the phase difference is enlarged, then the inductive behaviour prevails.

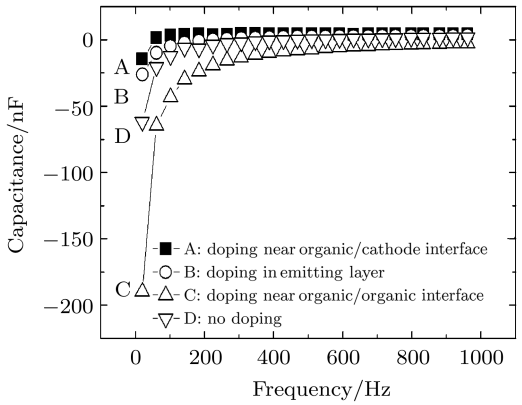


Fig. 6. The capacitance–frequency (C–F) characteristics measured under 12 V bias.

Figure 7 shows the C–F characteristics in the frequency range from 20 Hz to 1 kHz under the 2-V bias. One can see that all the devices do not exhibit NC at all, and capacitance C of the device ($C = C_{\rm g} + C_{\rm tr} + C_{\rm n}$, where $C_{\rm g}$ is the geometric capacitance) decreases with increasing frequency, approaching to the sum of geometric capacitance and additional capacitance at last in each case.

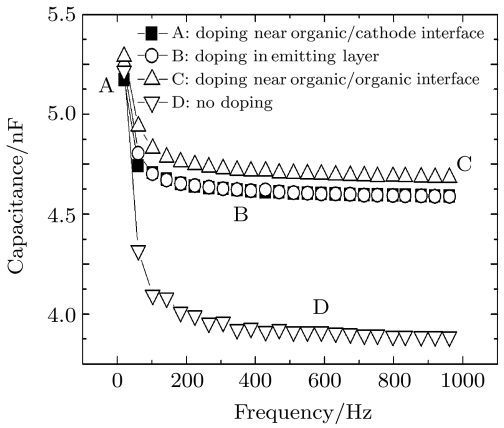


Fig. 7. The capacitance–frequency (C–F) characteristics measured under 2-V bias.

Term the response time $\tau_{\rm c}$ as $\tau_{\rm c} \propto 1/f$. Then the higher the frequency is, the shorter the response time is, hence the quicker the space charge redistribution forms. Since NC (inductive) is attributed to the lag between AC voltage and space charge redistribution produced by the accumulation of carriers near the organic/organic interface, the redistribution cannot be formed completely when the time for redistribution reduces, and then the lag effect is weaken. This results in the decreased inductive character. Extremely, when the response time is shorter than the transient time of carriers in the organic layer, NC disappears because the carriers driven by AC voltage cannot arrive at the organic/organic interface.

In the present experiment, the C–F characteristics are measured in the frequency region of 20 Hz to 1 kHz under the 2-V bias. It is hard to say how the bi-layer OLEDs will behave under the condition of low frequency and low bias similar to that of Garcia-Belmonte *et al.*[17,18] So a direct check of the problem, that whether the mechanism of NC due to the dynamic effect of interface states at the electrode/organic interface is correct or wrong in such a case may not be available. Nevertheless, from the results gained from doped bi-layer OLEDs, there should be no doubt that NC is closely related with the transport, distribution and recombination of carriers. Modulation on injection, transport, distribution and recombination of carriers can be realized by doping the same concentration and same volume dopants in the different regions of the light-emitting layer, keeping the electrode/organic interface structures of the device the same. In such a case, the density of states at the interface might be the same for the various devices. It is the doping region in the emitting layer that results in the different NC behaviours. Therefore, it can still be regarded that transport, distribution and recombination of carriers are the main factors leading to the NC behaviours in two bi-layer OLEDs.

4. Conclusions

In conclusion, the comparison of C–F and ϕ–F characteristics in the same frequency range and C–V and L–V characteristics under the same bias region reveals that NC originates from the inductive character due to transport, distribution and recombination of carriers in the bi-layer OLEDs. Doping in different regions of the light-emitting layer can change the injection and transport of carriers and the space charge distribution, which provides a possible way to separate the various factors affecting the NC behaviours of the devices.

References

[1] Campbell A J, Brandley D D C, Laubender J and Sokolowski M 1999 *J. Appl. Phys.* **86** 5004

[2] Bisquert J, Garcia-Belmonte G, Pitarch A and Bolink H J 2006 *Chem. Phys. Lett.* **422** 184

[3] Brütting W, Riel H, Beierlein T and Riess W 2001 *J. Appl. Phys.* **89** 1704

[4] Berleb S, Brütting W and Paasch G 2001 *Synthetic Metals* **122** 37

[5] Manna U, Kim H M, Gowtham M, Yi J, Sohn S and Jung D 2006 *Thin Solid Films* **495** 380

[6] Hulea I N, Van der Scheer R F J, Born H B, Langeveld-Voss B M W, van Dijken A and Brunner K 2003 *Appl. Phys. Lett.* **83** 1246

[7] Cvikl B, Kozelj M, Korošak D and Jecl R 2006 *J. Appl. Phys.* **99** 023704

[8] Gommans H H P, Kemerink M and Janssen R A J 2005 *Phys. Rev.* B **72** 235204

[9] Garcia-Belmonte G, Bolink H J and Bisquert J 2007 *Phys. Rev.* B **75** 085316

[10] Ehrenfreund E, Lungenschmied C, Dennler G, Neugebauer H and Sariciftci N S 2007 *Appl. Phys. Lett.* **91** 012112

[11] Castro F A, Bueno P R, Graeff C F O, Nüesch F, Zuppiroli L, Santos L F and Faria R M 2005 *Appl. Phys. Lett.* **87** 013505

[12] Pingree L S C, Scott B J, Russell M T, Marks T J and Hersam M C 2005 *Appl. Phys. Lett.* **86** 073509

[13] Pingree L S C, Russell M T, Marks T J and Hersam M C 2006 *J. Appl. Phys.* **100** 044502

[14] Pingree L S C, Russell M T, Marks T J and Hersam M C 2007 *Thin Solid Films* **515** 4783

[15] Tsai M N, Chang T C, Liu P T, Ko C W, Chen C J and Lo K M 2006 *Thin Solid Films* **498** 244

[16] Schmeits M 2007 *J. Appl. Phys.* **101** 084508

[17] Garcia-Belmonte G, Bisquert J, Bueno P R and Graeff C F O 2008 *Chem. Phys. Lett.* **455** 242

[18] Garcia-Belmonte G, Bisquert J, Bueno P R, Graeff C F O and Castro F 2009 *Synthetic Metals* **159** 480

[19] Zhan Y Q, Zhou J, Zhou Y C, Wu Y, Yang H, Li F Y, Ding X M and Hou X Y 2007 *Thin Solid Films* **515** 5449

[20] Choong V E, Park Y, Gao Y, Wehrmeister T, Müllen K, Hsieh B R and Tang C W 1996 *Appl. Phys. Lett.* **69** 1492

[21] Choong V E, Park Y, Shivaparan N, Tang C W and Gao Y 1997 *Appl. Phys. Lett.* **71** 1005

[22] Deshpande R S, Bulovic V and Forrest S R 1999 *Appl. Phys. Lett.* **75** 888

[23] Cheon K O and Shinar J 2004 *Appl. Phys. Lett.* **84** 1201

[24] Wu Y, Wu H R, Zhou Y C, Zhan Y Q, Zhou J, Ding X M and Hou X Y 2006 *Appl. Phys. Lett.* **88** 123512